
Binary Cumulative Encoding meets Time Series Forecasting

Andrei Chernov
Independent Researcher
Munich, Germany
chernov.andrey.998@gmail.com

Vitaliy Pozdnyakov
AIRI
Moscow, Russia
pozdnyakov@airi.net

Ilya Makarov
AIRI, ISP RAS, ITMO University
Moscow, Russia
makarov@airi.net

Abstract

Recent studies in time series forecasting have explored formulating regression via classification task. By discretizing the continuous target space into bins and predicting over a fixed set of classes, these approaches benefit from stable training, robust uncertainty modeling, and compatibility with modern deep learning architectures. However, most existing methods rely on one-hot encoding that ignores the inherent ordinal structure of the underlying values. As a result, they fail to provide information about the relative distance between predicted and true values during training. In this paper, we propose to address this limitation by introducing binary cumulative encoding (BCE), that represents scalar targets into monotonic binary vectors. This encoding implicitly preserves order and magnitude information, allowing the model to learn distance-aware representations while still operating within a classification framework. We propose a convolutional neural network architecture specifically designed for BCE, incorporating residual and dilated convolutions to enable fast and expressive temporal modeling. Through extensive experiments on benchmark forecasting datasets, we show that our approach outperforms widely used methods in both point and probabilistic forecasting, while requiring fewer parameters and enabling faster training.

1 Introduction

Time series forecasting plays a key role in decision-making across domains such as finance [1], healthcare [30], retail [5], and climate science [33]. While classical methods like ARIMA and Exponential Smoothing remain widely used in practice [14], recent advances increasingly favor deep learning approaches [18, 16], particularly in scenarios requiring high-precision forecasting [35].

A critical component of deep learning-based forecasting is data preprocessing. This typically includes normalization, min-max or mean scaling [29], Box-Cox transformation [14], and short-time Fourier transforms [10]. Recent studies [2, 20] have explored quantization, discretizing the continuous target space into fixed-size bins. Values are then represented as one-hot vectors, enabling a tokenized view of time series aligned with Transformer-style architectures. Empirical results suggest that such representations enhance performance, especially within Time Series Foundation Models [35].

However, one-hot encoding lacks ordinal awareness, treating bins as unrelated categories and ignoring relative distances—important cues for modeling temporal dynamics. To address this, we propose Binary Cumulative Encoding (BCE): a representation where all bins below (or equal to) the current value are activated. This monotonic encoding, previously applied to tabular data [11], preserves global ordinal structure and yields richer inputs for neural models. Figure 1 shows an example of BCE applied to a time series.

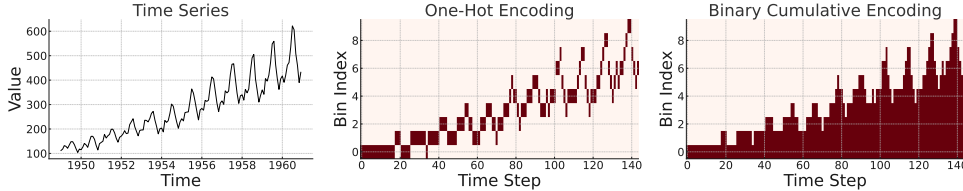


Figure 1: Visualization of different representations of time series data. **(left)** Original time series showing monthly airline passenger counts. **(center)** One-hot encoding of discretized values. **(right)** Binary Cumulative Encoding (BCE), where all bins less than or equal to the active bin are highlighted, preserving ordinal structure.

Choosing an appropriate neural architecture is another central design decision. RNNs, CNNs, and Transformers are commonly used, with Transformer-based models [35] excelling due to their capacity for long-range temporal modeling [32]. Yet, their nearly quadratic complexity with sequence length [31] poses practical challenges.

To overcome this, we introduce a CNN-based model that combines 2D and 1D convolutions to process BCE representations efficiently. This design reduces computational cost while preserving representational expressiveness. Moreover, BCE naturally supports probabilistic output by modeling distributions over bins—an ability often missing in standard CNN forecasting models.

We validate our method on the ProbTS benchmark [35], which includes diverse datasets from multiple domains. Our model consistently outperforms strong baselines in both point and probabilistic forecasting tasks.

The main contributions of this work are:

- A novel discrete representation, **Binary Cumulative Encoding (BCE)**, which captures ordinal and metric structure in time series.
- A lightweight convolutional model, **BinConv**, combining 2D and 1D convolutions to process BCE sequences efficiently.
- Extensive evaluation on the ProbTS benchmark, showing that our method achieves state-of-the-art results across multiple forecasting datasets.

2 Related Work

Classical and Deep Learning Methods for Time Series Forecasting. Classical models such as ARIMA, exponential smoothing, and vector autoregression are widely used for their simplicity and efficiency [14]. However, they often underperform on large-scale datasets exhibiting complex and nonlinear patterns, as shown in M4, M5, M6 forecasting competitions [24, 22, 25]. Deep learning approaches improve upon these by framing forecasting as a sequence-to-sequence problem using fixed context windows [18]. Recent developments like Time Series Foundation Models [17, 9, 8] leverage large-scale pretraining to generalize across domains, achieving strong results in both point and probabilistic forecasting [35].

Neural Network Architectures for Time Series Forecasting. Neural models vary in their trade-offs between accuracy, scalability, and speed. Transformer-based models such as PatchTST [26], TFT [19], and Informer [36] capture long-range dependencies well, but incur high computational costs due to their quadratic scaling with sequence length. Earlier RNN-based models like LSTM [13], GRU [6], and DeepAR [29] are more efficient at inference, though limited by their sequential nature, which hinders training parallelism. CNN-based

architectures such as TCN [4], DeepTCN [7], and ModernTCN [21] offer fast, parallel training and strong forecasting performance. Following this line, our CNN-based BinConv model balances accuracy and efficiency when used with BCE inputs.

Token-Based Representations of Time Series. Inspired by NLP, recent work reformulates time series forecasting as next-token prediction using discretization. Models like LLTime [12], TiMER [20], and Chronos [2] encode values as digits, patches, or bins. Gorishniy et al. [11] proposed piecewise linear encoding (PLE) for tabular data, preserving ordinal structure. Most models rely on one-hot encoding, which discards distance and order information between bins. This limits the ability to learn value relationships. In contrast, our BCE encoding captures both order and magnitude, improving learning while remaining compatible with token-based models.

Probabilistic Forecasting with Deep Learning Methods. Probabilistic forecasting offers both predictions and uncertainty. Deep learning models approach this via quantile regression (e.g., TFT, DeepAR), parametric output distributions (e.g., DeepTCN), or generative models like TimeGrad [27] and GRU-NVP [28]. While effective, generative approaches can be unstable and costly to train. Token-based models such as Chronos and TiMER enable probabilistic inference via sampling in discrete space. Our model adopts this approach using BCE, supporting both point and probabilistic forecasts through structured sampling.

3 Binary Cumulative Encoding

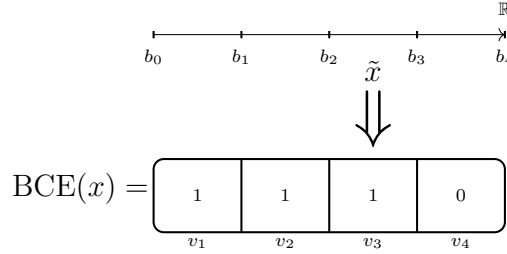


Figure 2: Example of BCE encoding for 4 bins.

The scale of time series can vary significantly, even within a single dataset. Therefore, before converting time series values into an encoding space, we apply normalization to map values into a quantized range. Similar to the Chronos model [2], we use the mean scaling technique [29], where each value is divided by the mean over a given context window. Specifically, we compute the scaled value as $\tilde{x} = x/s$, where $s = \frac{1}{C} \sum_{i=1}^C |x_i|$.

Next, we quantize the scaled time series as follows:

$$\begin{aligned} \text{BCE}(x) &= [v_1, \dots, v_D] \in \mathbb{R}^D \\ v_d &= \begin{cases} 0, & \tilde{x} < b_d \\ 1, & \tilde{x} \geq b_d \end{cases}, \end{aligned} \quad (1)$$

where b_d indicates a d -th bin in the original space. An example of construction of BCE is shown in Figure 2.

The interval from b_0 to b_D is uniformly split into D bins in a data-agnostic manner, where D , b_0 , and b_D are hyperparameters. In our experiments, we do not fine-tune these values per dataset and use fixed settings of $D = 1000$, $b_0 = -5$, and $b_D = 5$, unless stated otherwise. This quantization results in binary cumulative encoding of the form 111...100...0.

This type of encoding is not new in the context of tabular deep learning for numerical features [11]. However, unlike previous work, we not only transform the inputs using this scheme, but also forecast targets directly in the encoding space, as detailed in Section 4.2. After generating a forecast in the encoding space, we apply an inverse transformation by assigning the average value of the bin encoding, i.e., $\tilde{y} = (b_i + b_{i+1})/2$, where i is the index of the last

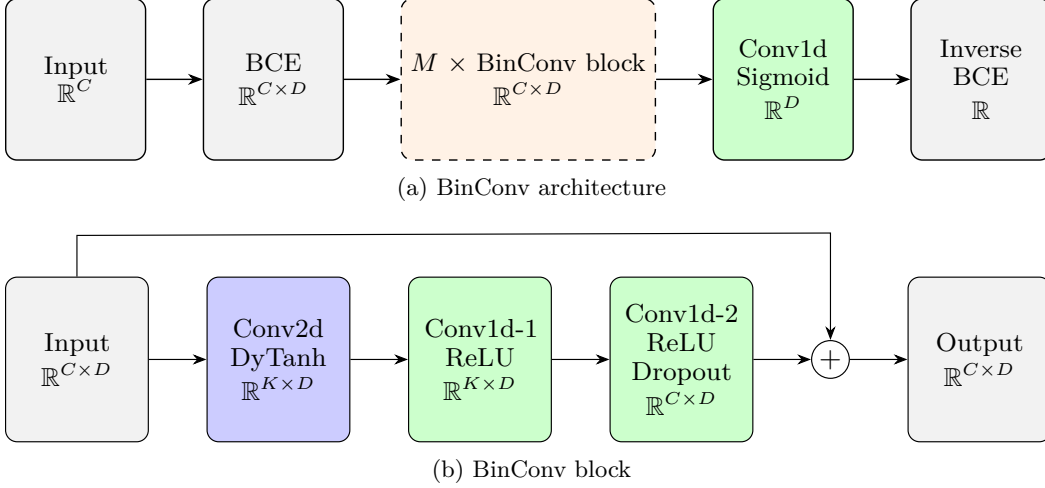


Figure 3: BinConv architecture. (a) First, we preprocess the time series using BCE. Then, the BinConv model is trained in the BCE space, and during forecasting, the inverse BCE transformation is applied to obtain predictions in the original space. BinConv consists of M stacked BinConv blocks followed by a final 1D convolution layer with a large kernel size. (b) Each BinConv block is the core component of the architecture, comprising three convolutional layers and a residual connection. The DyTanh activation function is used as a substitute for layer normalization. The output dimension of each BinConv block matches its input dimension.

1. Finally, to obtain the forecast in the original space, we reverse the mean scaling: $y = s \cdot \tilde{y}$. To the best of our knowledge, this approach is novel in the context of time series forecasting.

4 BinConv

4.1 Architecture

Table 1: Convolutional parameters used in BinConv.

Layer	Kernel Size	In/Out Channels	Groups
Conv2d	(C, s_1)	$1 / K$	1
Conv1d-1	s_2	K / K	K
Conv1d-2	s_2	K / C	K
Conv1d	s_3	$C / 1$	1

To model time series effectively in the discrete BCE space, the architecture must preserve ordinal relationships, support autoregressive forecasting, and maintain computational efficiency. To this end, we propose BinConv, a convolutional neural architecture that efficiently captures the local temporal and monotonic structure of BCE vectors by combining 2D and 1D convolutions.

The BinConv model consists of M convolutional blocks followed by a final convolutional layer with a sigmoid activation function, producing an output vector in the BCE space (see Figure 3a). For each convolution, we add padding on both sides to preserve output dimensionality. To preserve the cumulative structure of the BCE representation, we use ones for left padding and zeros for right padding. Notably, we do not use fully connected layers in the model. In fact, including fully connected layers degrades performance, as further discussed in Section 6.1.

Each BinConv block comprises three convolutional layers (see Figure 3b). The first is a 2D convolution with kernel size $(C, 3)$, where C corresponds to the context length. This layer

transforms the input matrix—obtained after applying BCE—into K one-dimensional vector representations, where K is the number of output channels and treated as a hyperparameter. Following the work of [37], we use the DyTanh activation function, which replaces layer normalization in our architecture.

Next, we apply two 1D convolutional layers with ReLU activation, followed by dropout after the second layer. Inspired by TCN architectures [4, 21], we employ depthwise convolution with the number of groups set to K , which significantly reduces computational cost without sacrificing performance 6.2. Each BinConv block is designed such that the input and output dimensions are identical. This allows the use of a residual connection as the final operation in the block, enabling the stacking of multiple BinConv blocks while mitigating the vanishing gradient problem. The main parameters of the model are listed in Table 1.

To train the model, we apply the binary cross-entropy loss to the model output. This approach is analogous to a multi-label classification setup, where each class is predicted independently using a "one-versus-all" scheme.

4.2 Forecasting

To forecast time series, we apply an autoregressive approach: forecasting at time step $t + 1$, appending the result to the context, then forecasting at $t + 2$, and so on. To do this, we need to transform the vector of sigmoid-activated outputs into a BCE. We interpret each component of the output as the success probability of an independent Bernoulli trial. Due to the design of the BCE, only sequences of the form $11 \dots 10 \dots 0$ are considered valid. Therefore, we normalize probability of each valid sequence by the total probability of all valid sequences, denoted as Z .

More formally, the probability of a valid encoding vector e_m , where the first m components are 1 and the remaining $D - m$ components are 0, is given by:

$$p(e_m) = \frac{\hat{p}(e_m)}{Z} = \frac{\left(\prod_{i=1}^m p_i\right) \left(\prod_{i=m+1}^D (1 - p_i)\right)}{\sum_{j=0}^D \left(\prod_{i=1}^j p_i \prod_{i=j+1}^D (1 - p_i)\right)}, \quad (2)$$

where p_i is the sigmoid output at position i .

Given these probabilities, we can either sample n trajectories autoregressively to obtain a probabilistic forecast, or take the argmax at each time step, which is faster but results in a point forecast. In Section 5, we show that the point estimates of the point and probabilistic forecasts do not differ significantly, and both outperform the point estimates of other models.

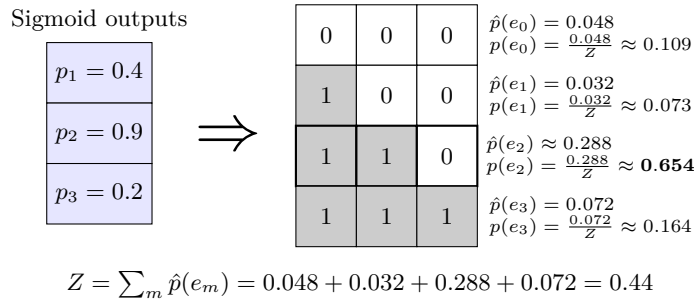


Figure 4: Converting the neural network output $[0.4, 0.9, 0.2]$ into a BCE, the most probable sequence is $[1, 1, 0]$.

5 Experiments

5.1 Setup

In this paper, our primary focus is on univariate forecasting. We evaluate performance on three univariate datasets: M4 Daily, M4 Weekly, and Tourism Monthly [23, 3]. The

prediction horizon H for each dataset is set to 14, 13, and 24, respectively. The context length is set to $C = 3H$ for all datasets.

We adopt the training and evaluation setup from [35]. Specifically, we train each model for 50 epochs, then select the best checkpoint based on performance on the training set, and report evaluation metrics on the test set. For all models, we used the Adam optimizer [15] for training. We compute CRPS using 20 quantile levels and 100 samples to assess the quality of probabilistic forecasts, and NMAE to evaluate point forecasting performance following to [35]. All computations were done on NVIDIA Tesla A10 22.5GB GPU RAM.

5.2 Results

We evaluated the performance of five different models: BinConv (our model), GRU-NVP, TimeGrad, and PatchTST, which are briefly described in Section 2. We also added simple linear model DLinear [34] for the comparison. For all baseline models, we use the optimal set of hyperparameters and normalization strategies provided by [35]. For BinConv, as discussed in Section 3, we used mean scaling before quantization. Mean scaling was applied independently to each sample, as the M4 datasets consist of diverse time series with varying scales. We did not fine-tune the BinConv model’s hyperparameters for each dataset, as it already demonstrated strong performance with the default configuration. The hyperparameters used across all datasets are summarized in Table 2.

Table 2: Default hyperparameters used for BinConv across all datasets. C denotes the context length.

Hyperparameter	Value
Number of bins (D)	1000
Minimum bin value (b_0)	-5
Maximum bin value (b_D)	5
Number of output channels (K)	C
Kernel size of 2D convolution in BinConv block (s_1)	3
Kernel size of 1D convolution in BinConv block (s_2)	3
Kernel size of final 1D convolution (s_3)	51
Number of BinConv blocks (M)	3
Dropout	0.35
Learning rate	0.001

The comparison between models is presented in Table 3. We trained and evaluated all models using five different random seeds and report the minimum, average, and maximum scores for each model. The metrics of BinConv are consistently better than those of the baseline models. Notably, the average scores of BinConv for both CRPS and NMAE are better than the best scores of all baselines.

Additionally, Table 4 compares the performance of BinConv when using argmax-based forecasting versus sampling-based forecasting (see Section 4.2 for details). While using point forecasting slightly degrades performance, it still outperforms all baseline models. We provide additional results on multivariate time-series datasets in Appendix C.

5.3 Efficiency of the Model

In Table 5, we report the total number of parameters for each model across all datasets. The DLinear model has significantly fewer parameters than the others, with BinConv being the second most parameter-efficient.

In Table 6, we present the average computation time during both training and inference for all models on the M4 Daily dataset. To obtain these results, we trained and evaluated all models using a batch size of 1, and computed the mean and standard deviation over all samples and epochs. As expected, DLinear is the fastest model during training, with BinConv being the second fastest.

Table 3: CRPS and NMAE results for all models. Each metric is reported as the average (AVG), minimum (MIN), and maximum (MAX) over 5 different seeds.

Dataset	Stat	DLinear		GRU-NVP		PatchTST		TimeGrad		BinConv	
		CRPS	NMAE	CRPS	NMAE	CRPS	NMAE	CRPS	NMAE	CRPS	NMAE
m4_daily	AVG	0.0440	0.0440	0.0714	0.0782	0.0438	0.0438	0.0587	0.0696	0.0327	0.0382
m4_weekly	AVG	0.1046	0.1046	0.0972	0.1062	0.1039	0.1039	0.1046	0.1283	0.0902	0.0972
tourism_monthly	AVG	0.2745	0.2745	0.3723	0.4536	0.2633	0.2633	0.2295	0.2968	0.1824	0.1955
m4_daily	MIN	0.0394	0.0394	0.0570	0.0649	0.0404	0.0404	0.0402	0.0475	0.0291	0.0341
m4_weekly	MIN	0.1007	0.1007	0.0916	0.1034	0.1020	0.1020	0.0800	0.0985	0.0851	0.0921
tourism_monthly	MIN	0.2595	0.2595	0.2880	0.3849	0.2281	0.2281	0.1993	0.2596	0.1777	0.1911
m4_daily	MAX	0.0506	0.0506	0.1196	0.1259	0.0476	0.0476	0.0933	0.1077	0.0366	0.0427
m4_weekly	MAX	0.1072	0.1072	0.1006	0.1085	0.1078	0.1078	0.1718	0.2121	0.0981	0.1055
tourism_monthly	MAX	0.3077	0.3077	0.5799	0.5399	0.2888	0.2888	0.2500	0.3186	0.1892	0.2012

Table 4: Comparison of BinConv performance using sampling versus argmax forecasting. Each metric is reported as the average (AVG), minimum (MIN), and maximum (MAX) over 5 different seeds.

Dataset	Stat	Argmax		Sampling	
		CRPS	NMAE	CRPS	NMAE
m4_daily	AVG	0.0371	0.0371	0.0327	0.0382
m4_weekly	AVG	0.0975	0.0975	0.0902	0.0972
tourism_monthly	AVG	0.1961	0.1961	0.1824	0.1955
m4_daily	MIN	0.0348	0.0348	0.0291	0.0341
m4_weekly	MIN	0.0927	0.0927	0.0851	0.0921
tourism_monthly	MIN	0.1916	0.1916	0.1777	0.1911
m4_daily	MAX	0.0387	0.0387	0.0366	0.0427
m4_weekly	MAX	0.1049	0.1049	0.0981	0.1055
tourism_monthly	MAX	0.2013	0.2013	0.1892	0.2012

During inference, PatchTST is the fastest model because it is non-autoregressive and predicts the entire forecast horizon in a single forward pass. DLinear ranks second, followed by BinConv and GRU-NVP, which exhibit similar inference speeds—approximately twice as slow as PatchTST. TimeGrad is significantly slower than all other models.

Using point (argmax-based) forecasting instead of sampling improves inference speed by approximately 25%. However, the difference is not dramatic, as sampling is implemented by duplicating the input N times, where N is the number of samples. This allows all N samples to be processed in a single batch.

Table 5: Total number of parameters (in thousands) per method and dataset.

Dataset	DLinear	BinConv	PatchTST	TimeGrad	GRU-NVP
m4_daily	1.204	20.173	47.470	107.434	141.108
m4_weekly	1.040	17.680	43.725	107.434	141.108
tourism_monthly	3.504	54.013	155.288	107.434	141.108

6 Ablation Study

In this section, we conduct ablation studies to better understand the contribution of core components in our model architecture. Specifically, we investigate the effect of replacing the final layer with a fully connected layer (Section 6.1), substituting Depthwise convolution layers in the BinConv block with standard convolution layers (Section 6.2), and using DyTanh instead of layer normalization (Section 6.3). Each component is modified independently, while the rest of the architecture and hyperparameters remain unchanged from the standard BinConv model. During the prediction stage, we used probabilistic forecasting to measure the difference between both probabilistic and point estimates. To save computation time,

Table 6: Mean and standard deviation of time (in seconds) to process a single sample for the M4 Daily dataset.

Phase	DLinear	BinConv		PatchTST	TimeGrad	GRU-NVP
		Argmax	Sampling			
Train	0.0123 ± 0.0026	0.0284 ± 0.0043	0.0284 ± 0.0043	0.0381 ± 0.0049	0.0450 ± 0.0063	0.0362 ± 0.0048
Test	0.0755 ± 0.0016	0.09684 ± 0.00306	0.12788 ± 0.0017	0.0547 ± 0.0021	2.7723 ± 0.0365	0.1239 ± 0.0086

we ran all modified models using a single seed and compared their performance with the average performance of BinConv.

Table 7: Comparison between the standard BinConv model and its architectural variations. The notation **w/** indicates that the standard BinConv is modified by replacing a specific component: **w/ FC Layer** uses a fully connected layer instead of the final convolution, **w/ Standard Conv** replaces Depthwise convolutions with standard ones, and **w/ LayerNorm** substitutes DyTanh with layer normalization.

Dataset	BinConv		w/ FC Layer		w/ Standard Conv		w/ LayerNorm	
	CRPS	NMAE	CRPS	NMAE	CRPS	NMAE	CRPS	NMAE
m4_daily	0.0327	0.0382	0.0411	0.0468	0.0292	0.0343	0.0311	0.0365
m4_weekly	0.0902	0.0972	0.0870	0.0943	0.1028	0.1112	0.0847	0.0921
tourism_monthly	0.1824	0.1955	0.1756	0.1910	0.1801	0.1945	0.1761	0.1889

Table 8: Number of parameters (in thousands) for the standard BinConv model and its architectural variations. See the caption of Table 7 for the explanation of the column notation.

Dataset	BinConv	w/ FC Layer	w/ Standard Conv	w/ LayerNorm
m4_daily	20.173	1019.540	51.679	20.170
m4_weekly	17.680	1017.164	44.830	17.677
tourism_monthly	54.013	1052.210	146.899	54.010

6.1 Using Linear Layer in the Output

When designing the BinConv architecture, we deliberately avoided using fully connected layers. There are two main reasons for this. First, fully connected layers introduce significantly more trainable parameters compared to convolutional layers, especially considering that the our model’s output lies in a high-dimensional space. Second, because of the design of BCE and the way we compute the loss during training, using a fully connected layer, especially when it serves as the final layer, may limit BinConv’s ability to forecast values on the test set that fall outside the range observed during training. We elaborate on this in detail in Appendix B.

Nevertheless, since fully connected layers are a popular design choice, we evaluate the performance of BinConv when a fully connected layer is used as the final layer. To implement this variant, we replace the final 1D convolutional layer as follows. The output of the BinConv blocks is a vector $h \in \mathbb{R}^{C \times D}$, where C is the context length and D is the number of bins. We first average h over the context dimension, resulting in a vector $\bar{h} \in \mathbb{R}^D$. A fully connected layer is then applied to map \mathbb{R}^D to \mathbb{R}^D .

In Table 7, we report the evaluation metrics for this variant in the column labeled “w/ FC Layer”. As we expected, the performance degrades significantly. Furthermore, as shown in Table 8, adding a fully connected layer dramatically increases the number of trainable parameters, making the model less efficient.

6.2 Using Depthwise instead of Standard Convolution

Depthwise convolution is a form of convolution in which each input channel is convolved independently with its own filter. As a result, it requires significantly fewer convolutional

kernels, which improves the model’s computational efficiency. In our model, we use this type of convolution in the BinConv block for 1D operations.

The performance of BinConv with standard 1D convolutional layers in place of depthwise layers is reported in Table 7, in the column labeled “w/ Standard Conv”. Replacing depthwise convolutions with standard ones does not improve performance, but it does reduce model efficiency, as shown in Table 8.

6.3 Using Layer Normalization instead of DyTanh

In [37], the authors proposed using DyTanh instead of layer normalization for transformer models. They demonstrated empirically that it yields comparable or better results in computer vision (CV) and natural language processing (NLP) tasks.

Inspired by this finding, we replace layer normalization with DyTanh in BinConv. In this section, we assess whether substituting DyTanh with traditional layer normalization followed by a ReLU activation affects performance. As shown in Table 7, the performance of this model variant is similar to or better than that of the standard BinConv, indicating that layer normalization is also a valid choice for our architecture. The number of parameters is also comparable (Table 8); DyTanh introduces only one additional parameter compared to the normalization layer, which is a negligible difference.

7 Conclusion

In this paper, we proposed using Binary Cumulative Encoding (BCE) as a discrete quantization technique for time series, and we introduced BinConv, a convolutional architecture specifically designed for efficient processing of BCE vectors. Extensive evaluation on the publicly available ProbTS benchmark demonstrates that our method achieves state-of-the-art performance across diverse domains.

Despite these promising results, our method has several limitations. First, BCE discretizes time series values, which requires approximating the precision of continuous data and can result in information loss. Second, selecting the number of bins introduces a trade-off: too few bins reduce representational fidelity, while too many increase computational complexity. Third, the current design is limited to univariate time series, which necessitates modeling each variable independently and prevents capturing cross-series interaction.

Future directions for this work include evaluating the generalization capability of our method in a Time Series Foundation Model setting, where the model is tested on previously unseen datasets. Another promising avenue is to extend the BinConv architecture to support multivariate time series by modeling interactions between components. Additionally, our approach could be applied to other time series tasks, such as imputation, anomaly detection, and classification.

References

- [1] Ryo Akita et al. “Deep learning for stock prediction using numerical and textual information”. In: *2016 IEEE/ACIS 15th International Conference on Computer and Information Science (ICIS)*. IEEE. 2016, pp. 1–6.
- [2] Abdul Fatir Ansari et al. “Chronos: Learning the Language of Time Series”. In: *Transactions on Machine Learning Research* (2024). ISSN: 2835-8856. URL: <https://openreview.net/forum?id=gerNCVqqtR>.
- [3] George Athanasopoulos et al. “The tourism forecasting competition”. In: *International Journal of Forecasting* 27.3 (2011), pp. 822–844.
- [4] Shaojie Bai, J Zico Kolter, and Vladlen Koltun. “An empirical evaluation of generic convolutional and recurrent networks for sequence modeling”. In: *arXiv preprint arXiv:1803.01271* (2018).
- [5] Kasun Bandara et al. “Sales demand forecast in e-commerce using a long short-term memory neural network methodology”. In: *Neural Information Processing: 26th International Conference, ICONIP 2019, Sydney, NSW, Australia, December 12–15, 2019, Proceedings, Part III* 26. Springer. 2019, pp. 462–474.
- [6] Zhengping Che et al. “Recurrent neural networks for multivariate time series with missing values”. In: *Scientific reports* 8.1 (2018), p. 6085.
- [7] Yitian Chen et al. “Probabilistic forecasting with temporal convolutional neural network”. In: *Neurocomputing* 399 (2020), pp. 491–501.
- [8] Luke Nicholas Darlow et al. “DAM: Towards a Foundation Model for Forecasting”. In: *The Twelfth International Conference on Learning Representations*. 2024. URL: <https://openreview.net/forum?id=4NhMhElWqP>.
- [9] Abhimanyu Das et al. “A decoder-only foundation model for time-series forecasting”. In: *Forty-first International Conference on Machine Learning*. 2024.
- [10] Łukasz Furman et al. “Short-time Fourier transform and embedding method for recurrence quantification analysis of EEG time series”. In: *The European Physical Journal Special Topics* 232.1 (2023), pp. 135–149.
- [11] Yury Gorishniy, Ivan Rubachev, and Artem Babenko. “On embeddings for numerical features in tabular deep learning”. In: *Advances in Neural Information Processing Systems* 35 (2022), pp. 24991–25004.
- [12] Nate Gruver et al. “Large language models are zero-shot time series forecasters”. In: *Advances in Neural Information Processing Systems* 36 (2023), pp. 19622–19635.
- [13] Sepp Hochreiter and Jürgen Schmidhuber. “Long short-term memory”. In: *Neural computation* 9.8 (1997), pp. 1735–1780.
- [14] Rob J Hyndman and George Athanasopoulos. *Forecasting: principles and practice*. OTexts: Melbourne, Australia. OTexts.com/fpp3. Accessed on May 2025. OTexts, 2021.
- [15] DP Kingma. “Adam: a method for stochastic optimization”. In: *arXiv: 1412.6980* (2015).
- [16] Wenxiang Li and KL Eddie Law. “Deep learning models for time series forecasting: a review”. In: *IEEE Access* (2024).
- [17] Yuxuan Liang et al. “Foundation models for time series analysis: A tutorial and survey”. In: *Proceedings of the 30th ACM SIGKDD conference on knowledge discovery and data mining*. 2024, pp. 6555–6565.
- [18] Bryan Lim and Stefan Zohren. “Time-series forecasting with deep learning: a survey”. In: *Philosophical Transactions of the Royal Society A* 379.2194 (2021), p. 20200209.
- [19] Bryan Lim et al. “Temporal fusion transformers for interpretable multi-horizon time series forecasting”. In: *International Journal of Forecasting* 37.4 (2021), pp. 1748–1764.
- [20] Yong Liu et al. “Timer: generative pre-trained transformers are large time series models”. In: *Proceedings of the 41st International Conference on Machine Learning*. 2024, pp. 32369–32399.
- [21] Donghao Luo and Xue Wang. “Moderntcn: A modern pure convolution structure for general time series analysis”. In: *The twelfth international conference on learning representations*. 2024, pp. 1–43.

- [22] Spyros Makridakis, Evangelos Spiliotis, and Vassilios Assimakopoulos. “M5 accuracy competition: Results, findings, and conclusions”. In: *International Journal of Forecasting* 38.4 (2022), pp. 1346–1364.
- [23] Spyros Makridakis, Evangelos Spiliotis, and Vassilios Assimakopoulos. “The M4 Competition: 100,000 time series and 61 forecasting methods”. In: *International Journal of Forecasting* 36.1 (2020), pp. 54–74.
- [24] Spyros Makridakis, Evangelos Spiliotis, and Vassilios Assimakopoulos. “The M4 Competition: Results, findings, conclusion and way forward”. In: *International Journal of forecasting* 34.4 (2018), pp. 802–808.
- [25] Spyros Makridakis et al. “The M6 forecasting competition: Bridging the gap between forecasting and investment decisions”. In: *International Journal of Forecasting* (2024).
- [26] Yuqi Nie et al. “A Time Series is Worth 64 Words: Long-term Forecasting with Transformers”. In: *The Eleventh International Conference on Learning Representations*. 2023. URL: <https://openreview.net/forum?id=Jbdc0vT0col>.
- [27] Kashif Rasul et al. “Autoregressive denoising diffusion models for multivariate probabilistic time series forecasting”. In: *International conference on machine learning*. PMLR. 2021, pp. 8857–8868.
- [28] Kashif Rasul et al. “Multivariate Probabilistic Time Series Forecasting via Conditioned Normalizing Flows”. In: *International Conference on Learning Representations*. 2021. URL: <https://openreview.net/forum?id=WlGQBFuVRv>.
- [29] David Salinas et al. “DeepAR: Probabilistic forecasting with autoregressive recurrent networks”. In: *International journal of forecasting* 36.3 (2020), pp. 1181–1191.
- [30] Yan Song et al. “Distributed attention-based temporal convolutional network for remaining useful life prediction”. In: *IEEE Internet of Things Journal* 8.12 (2020), pp. 9594–9602.
- [31] Yi Tay et al. “Efficient transformers: A survey”. In: *ACM Computing Surveys* 55.6 (2022), pp. 1–28.
- [32] Ashish Vaswani et al. “Attention is all you need”. In: *Advances in neural information processing systems* 30 (2017).
- [33] Nur’atiah Zaini et al. “A systematic literature review of deep learning neural network for time series air quality forecasting”. In: *Environmental Science and Pollution Research* (2022), pp. 1–33.
- [34] Ailing Zeng et al. “Are transformers effective for time series forecasting?” In: *Proceedings of the AAAI conference on artificial intelligence*. Vol. 37. 9. 2023, pp. 11121–11128.
- [35] Jiawen Zhang et al. “ProbTS: Benchmarking point and distributional forecasting across diverse prediction horizons”. In: *Advances in Neural Information Processing Systems* 37 (2024), pp. 48045–48082.
- [36] Haoyi Zhou et al. “Informer: Beyond efficient transformer for long sequence time-series forecasting”. In: *Proceedings of the AAAI conference on artificial intelligence*. Vol. 35. 12. 2021, pp. 11106–11115.
- [37] Jiachen Zhu et al. “Transformers without normalization”. In: *arXiv preprint arXiv:2503.10622* (2025).

A Evaluation on Additional Datasets

In this section, we report results for long-term forecasting on several datasets commonly used in the research community: ETTh1, ETTh2, ETTm1, ETTm2, and Illness [35]. For baseline models, we used the optimal set of hyperparameters from [35], while for BinConv we used the default configuration without any fine-tuning (see Table 10). The context length and prediction length were set to 36 for the Illness dataset and 96 for the others.

For each dataset and model, we ran only a single seed due to the computational cost of evaluation—particularly for models like CSDI and TimeGrad, which can require up to 20 hours for training and evaluation. All datasets are multivariate and contain 7 variables each. Since BinConv currently supports only univariate forecasting, and extending it to multivariate settings is left for future work, we forecasted each time series independently using the sampling procedure described in Section 4.2. Table 11 reports the total number of parameters for each model. BinConv is less parameter-efficient in the multivariate setting than in the univariate case, as it maintains a separate model for each time series in the dataset.

In Table 9, we report CRPS and NMAE for all baseline models and BinConv. As there is no clear winner across all datasets, we additionally report model rankings for both metrics in Table 12. Rankings were calculated based on relative performance: the best-performing model on each dataset received rank 1, the second-best received rank 2, and so on.

Despite the fact that BinConv’s hyperparameters were not tuned and the model is not specifically designed for multivariate forecasting, it achieved the best average rank based on the CRPS metric and the second-best rank based on the NMAE metric.

Table 9: Forecasting performance (CRPS and NMAE) across different models and datasets. All datasets use context length 96 and prediction length 96 (except Illness, it uses 36 for both).

Dataset	DLinear		PatchTST		GRU-NVP		TimeGrad		CSDI		BinConv	
	CRPS	NMAE	CRPS	NMAE	CRPS	NMAE	CRPS	NMAE	CRPS	NMAE	CRPS	NMAE
ETTh1	0.3339	0.3339	0.3218	0.3218	0.3435	0.4383	0.2930	0.3867	0.3830	0.4871	0.2969	0.3201
ETTh2	0.2319	0.2319	0.1763	0.1763	0.2623	0.3100	0.2059	0.2574	0.2291	0.3004	0.1709	0.1853
ETTh1	0.2663	0.2663	0.2681	0.2681	0.4029	0.5018	0.4201	0.5153	0.2397	0.3124	0.2922	0.3141
ETTh2	0.1431	0.1431	0.1337	0.1337	0.2106	0.2618	0.1595	0.1930	0.1116	0.1413	0.1329	0.1456
Illness	0.1869	0.1869	0.1103	0.1103	0.0750	0.0828	0.0643	0.0868	0.3077	0.3237	0.1187	0.1447

Table 10: Default hyperparameters used for BinConv across long term datasets. C denotes the context length.

Hyperparameter	Value
Number of bins (D)	500
Minimum bin value (b_0)	−5
Maximum bin value (b_D)	5
Number of output channels (K)	C
Kernel size of 2D convolution in BinConv block (s_1)	3
Kernel size of 1D convolution in BinConv block (s_2)	3
Kernel size of final 1D convolution (s_3)	51
Number of BinConv blocks (M)	3
Dropout	0.35
Learning rate	0.001

B Qualitative Analysis

B.1 The Ability to Capture the Trend

In Section 6.1, we mentioned that replacing the convolutional layer with a fully connected layer as the final layer results in the model’s inability to forecast values outside the training

Table 11: Number of trainable parameters (in thousands) for each model across datasets.

Dataset	DLinear	PatchTST	GRU-NVP	TimeGrad	CSDI	BinConv
ETTh1	130.368	148.240	209.059	302.071	430.001	637.663
ETTh2	18.624	33.616	414.983	115.815	430.001	637.663
ETTm1	130.368	1347.872	264.263	297.079	430.001	637.663
ETTm2	18.624	1347.872	412.459	70.199	430.001	637.663
Illness	2.664	57.836	588.039	69.623	430.001	103.063

Table 12: Model rankings by NMAE and CRPS (lower is better). Rank 1 = best performance. Averages are computed across all datasets.

Dataset	DLinear	PatchTST	GRU-NVP	TimeGrad	CSDI	BinConv
NMAE Rank						
ETTh1	3	2	5	4	6	1
ETTh2	3	1	6	4	5	2
ETTm1	1	2	5	6	3	4
ETTm2	3	1	6	5	2	4
Illness	5	3	1	2	6	4
Average	3.0	1.8	4.8	4.2	4.4	3.0
CRPS Rank						
ETTh1	4	3	5	1	6	2
ETTh2	5	2	6	3	4	1
ETTm1	2	3	5	6	1	4
ETTm2	4	3	6	5	1	2
Illness	5	3	2	1	6	4
Average	4.0	2.8	4.8	3.2	3.6	2.6

range. This occurs because, unlike convolutional layers, fully connected layers do not share weights. As a result, each component of the output vector is associated with its own set of learnable parameters that influence only that component.

A direct consequence of this is that if the last K components of the labels during training are always zero, the network can trivially learn to predict zeros for those components, thereby failing to extrapolate any upward or downward trends.

To illustrate this, we generated a synthetic dataset with a linear trend:

$$s_t = (100 + 1.5 \cdot t)(1 + \sigma_t), \quad t = 0, 1, \dots, T - 1,$$

where $\sigma_t \sim \mathcal{N}(0, 10^{-4})$. We set $T = 144$, using the first 120 values for training and the remaining 24 for testing. We then trained both the original BinConv and a variant with a fully connected output layer (BinConv w/ FC), and forecasted the final 48 values. The hyperparameters used for BinConv are provided in Table 13. Context length was set to 72, and the prediction horizon to 24. The BinConv w/ FC variant was constructed as described in Section 6.1. For simplicity, during forecasting, we did not sample from the output distribution but instead used the BinConv Argmax procedure from Section 4.2.

Figure 5 shows the forecast for the last 48 values alongside the ground truth. As the test phase begins, BinConv w/ FC outputs a constant value corresponding to the maximum it observed during training, failing to capture the trend. In contrast, BinConv successfully extrapolates the linear trend and achieves accurate forecasts.

B.2 The Ability to Capture the Seasonality

In this section, we illustrate that BinConv is capable of capturing seasonality. To demonstrate this, we generate a synthetic dataset over discrete time steps $t = 0, 1, \dots, T - 1$. The data

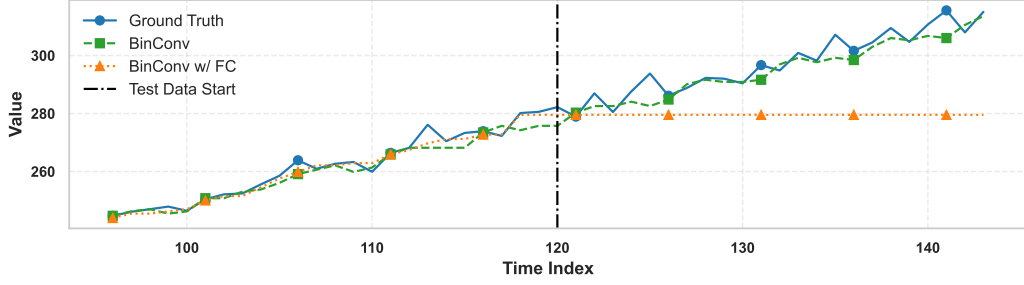


Figure 5: Forecast comparison of BinConv and BinConv w/ FC on synthetic linear trend data. The vertical line marks the start of the test data. BinConv w/ FC fails to forecast values beyond those seen during training.

Table 13: Model Parameters for Synthetic Datasets

Parameter	Value
Learning Rate ($1r$)	0.1
Dropout	0.0
Number of Bins	500
Minimum bin value (b_0)	-2
Maximum bin value (b_D)	2
Number of Blocks (K)	1
Kernel Size of 2D convolution in BinConv block (s_1)	3
Kernel Size of 1D convolution in BinConv block (s_2)	3
Kernel Size of final 1D convolution (s_3)	51
Number of Filters (2D)	72
Number of Filters (1D)	72

follows a sinusoidal seasonal pattern with additive Gaussian noise:

$$s_t = 100 + A \cdot \sin\left(\frac{2\pi t}{P}\right) + \varepsilon_t, \quad t = 0, 1, \dots, T-1,$$

where $A = 10$, $P = 12$, $\varepsilon_t \sim \mathcal{N}(0, 1)$, and $T = 144$. The model hyperparameters are reported in Table 13. The context length is set to 72 and the prediction horizon to 24. The model was trained on the first 120 data values and used to forecast the last 48. The first 24 test values were seen during training, while the final 24 values were not.

Figure 6 presents the forecast results, which demonstrate that BinConv successfully captures the seasonal structure of the data.

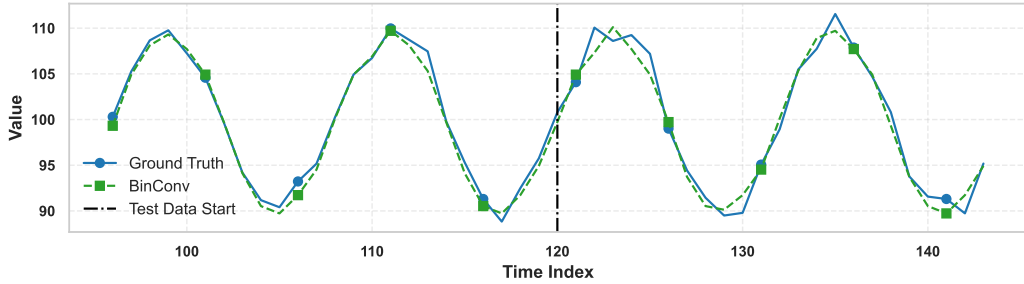


Figure 6: Comparison of forecasting methods against observed values. The vertical line indicates the start of the test data.

C Evaluation Metrics

In our experiments, we employ the normalized mean absolute error (NMAE) for evaluating point forecasts, and the continuous ranked probability score (CRPS) for evaluating probabilistic forecasts. These metrics are widely adopted in time series forecasting research [35, 7, 2, 28].

NMAE is defined as:

$$\text{NMAE} = \frac{\sum_{k=1}^K \sum_{t=1}^T |x_t^k - \hat{x}_t^k|}{\sum_{k=1}^K \sum_{t=1}^T |x_t^k|},$$

where K denotes the dimensionality of the multivariate time series (and is 1 in the univariate case), T is the prediction length (i.e., forecasting horizon), x_t^k is the observed target value, and \hat{x}_t^k is the predicted value.

CRPS is given by:

$$\text{CRPS}(F^{-1}, x) = \int_0^1 2\Lambda_\alpha(F^{-1}(\alpha), x) d\alpha,$$

where $\Lambda_\alpha(q, z)$ is the quantile loss function at quantile level α , defined as:

$$\Lambda_\alpha(q, z) := (\alpha - \mathbb{I}\{z < q\})(z - q),$$

and $\mathbb{I}\{z < q\}$ is the indicator function, which equals 1 if $z < q$ and 0 otherwise.

To approximate CRPS for discrete data, we use 19 quantile levels ranging from 0.05 to 0.95 in steps of 0.05, leading to:

$$\text{CRPS}(F^{-1}, x) \approx \sum_{i=1}^{19} 2\Lambda_{i \times 0.05}(F^{-1}(i \times 0.05), x).$$

To estimate the empirical quantile function F^{-1} , we sample 100 forecasts. For probabilistic forecasting models, the point forecast is computed as the average of these sampled forecasts. In contrast, for point forecasting models, all quantiles are presented by the single predicted value. In this case, it can be shown that the NMAE is equivalent to the CRPS, leading to identical values for both metrics.